Supporting Information

Spin-Forbidden Hydrogen Atom Transfer Reactions in a Cobalt Biimidazoline System

Virginia W. Manner,[§,ø] Alex D. Lindsay,[§] Elizabeth A. Mader,[§,†]

Jeremy N. Harvey,[‡,*] and James M. Mayer[§,*]

[§] *University of Washington, Department of Chemistry, Campus Box 351700,*

Seattle, WA 98195-1700, mayer@chem.washington.edu

[‡] *Centre for Computational Chemistry and School of Chemistry, University of Bristol,*

Cantock's Close, Bristol, UK BS8 1TS, jeremy.harvey@bristol.ac.uk

Contents

ø Current address: Explosives Applications and Special Projects, Los Alamos National Laboratory, MS C920, Los Alamos, NM, 87545; vwmanner@lanl.gov

† Current address: Chemical Sciences and Engineering Division, Argonne National Laboratory, 9700 South Cass Ave, CSE/200, Argonne, IL, 60439-4837; mader@anl.gov.

I. Co^{III}Hbim + H$_2$Q $\rightleftharpoons$ Co^{III}Hbim|H$_2$Q pre-equilibrium

The formation of a hydrogen-bonded complex between **Co^{III}Hbim** and **H$_2$Q** (eq S1) is indicated by a large absorbance change upon mixing the two reagents. The absorbance drop at 586 nm was measured in various experiments, with $[\text{H}_2\text{Q}]_{\text{total}} = 5.9 – 407$ mM and $[\text{Co}^{III}\text{Hbim}]_{\text{total}} = 0.28 – 0.76$ mM. At high $[\text{H}_2\text{Q}]$ (≥ 346 mM), formation of the complex is complete, yielding an estimated extinction coefficient of the complex, $\varepsilon_{586,\text{CoIII-H2Q}} \sim 350$ M^{-1} cm^{-1}. At a given concentration of **H$_2$Q**, solutions of $0.4 – 1$ mM **Co^{III}Hbim** gave a constant (within 12%) ratio of **Co^{III}Hbim|H$_2$Q** to **Co^{III}Hbim**, confirming the 1:1 stoichiometry of the adduct. These data give K_{6S} for formation of the hydrogen bonded complex as 14 ± 7 M^{-1} (Figure S1), with the large error bar reflecting complications from some decomposition or other reactivity on the timescale of the measurements.
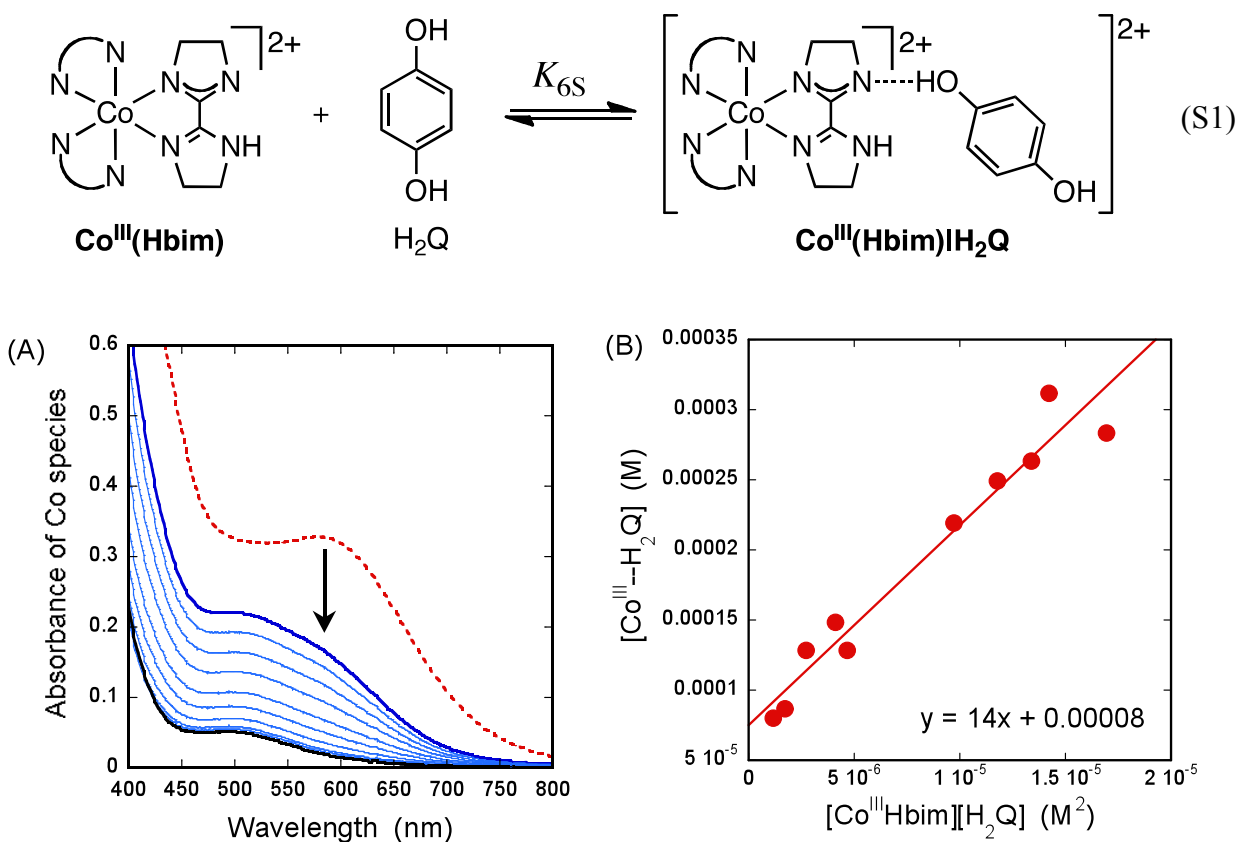

Co^{III}(Hbim)   H$_2$Q   Co^{III}(Hbim)|H$_2$Q   (S1)

Figure S1. (a) UV-Visible spectra for **Co^{III}Hbim** (0.51 mM, dotted red line), **Co^{III}Hbim--H$_2$Q** immediately after mixing (0.51 mM, uppermost solid blue line), and the final absorbance after the reaction is complete (bottom solid black line). (b) Plot of $[\text{Co}^{III}\text{Hbim}][\text{H}_2\text{Q}]$ *vs.* $[\text{Co}^{III}\text{Hbim}$--$\text{H}_2\text{Q}]$, with slope K_{6S}.

II. Table of rates for $Co^{III}Hbim + H_2Q$.

Table S1. Initial rates (first 15%) for $Co^{III}Hbim + H_2Q$

$[Co^{III}Hbim]$ (M)	$[H_2Q]$ (M)	$d[Co^{III}]/dt$ (M s^{-1})
0.00043	0.0464	1.7×10^{-8}
0.00074	0.0464	6.8×10^{-8}
0.0011	0.0464	1.3×10^{-7}
0.00037	0.0532	2.2×10^{-8}
0.00065	0.0532	7.0×10^{-8}
0.0010	0.0532	1.8×10^{-7}

III. Table and Figures for $Co^{III}Dbim + D_2Q$.

Table S2. Rates of first 15% of reactions for $Co^{III}Hbim + H_2Q$ *vs*. $Co^{III}Dbim + D_2Q$

$[Co^{III}Hbim]$ (M) ($[Co^{III}Dbim]$)	$[H_2Q]$ ($[D_2Q]$) (M)	$d[Co^{III}]/dt$ (M s^{-1}) ($d[Co^{III}(D)]/dt$)	~k_H/k_D
0.00064 (0.00064)	0.0300 (0.0299)	5.0×10^{-8} (2.8×10^{-8})	1.8
0.00064 (0.00064)	0.0568 (0.0589)	6.9×10^{-8} (5.0×10^{-8})	1.4
0.00064 (0.00063)	0.0717 (0.0709)	7.0×10^{-8} (5.4×10^{-8})	1.3
0.00063 (0.00063)	0.0778 (0.0785)	8.0×10^{-8} (6.2×10^{-8})	1.3
			Avg $\approx$ 1.5
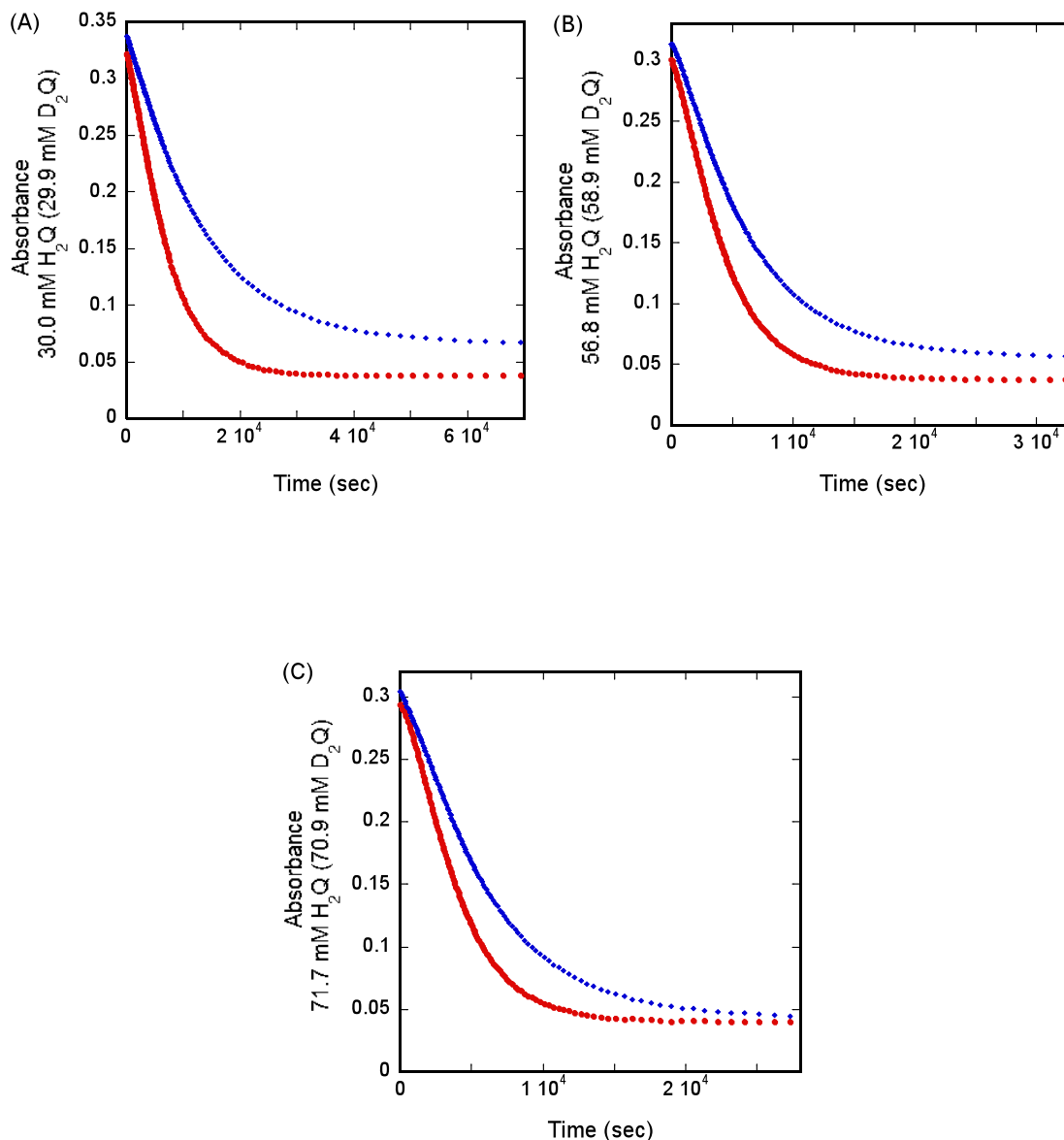
Figure S2. Absorbance at 586 nm *vs.* time (sec) for the UV-visible spectra of the reaction of **Co^{III}Hbim** + **H$_2$Q**, where the absorbance change is due to the decrease in {**Co^{III}Hbim** + **Co^{III}Hbim-H$_2$Q**}. (A) 0.64 mM **Co^{III}Hbim** + 30.0 mM **H$_2$Q** (red trace) and 0.64 mM **Co^{III}Dbim** + 29.9 mM **D$_2$Q** (blue trace). (B) 0.64 mM **Co^{III}Hbim** + 56.8 mM **H$_2$Q** (red trace) and 0.64 mM **Co^{III}Dbim** + 58.9 mM **D$_2$Q** (blue trace). (C) 0.64 mM **Co^{III}Hbim** + 71.7 mM **H$_2$Q** (red trace) and 0.63 mM **Co^{III}Dbim** + 70.9 mM **D$_2$Q** (blue trace).

IV. Complications with Initial Rate Data for the Reaction of $Co^{III}Hbim + H_2Q$

Monitoring the reaction of $Co^{III}Hbim$ and H_2Q by UV-Visible spectroscopy shows a rapid decrease in absorbance (due to formation of the hydrogen-bonded complex, $Co^{III}Hbim\text{--}H_2Q$), followed by slow reactivity to give $Co^{II}H_2bim$ over the course of hours. After the initial drop in absorbance, the optical spectra show that solutions of $Co^{III}Hbim\text{--}H_2Q + H_2Q$ proceed over the course of hours to an equilibrium mixture with $Co^{II}H_2bim$ and BQ (which is confirmed quantitatively by ^1H NMR). Attempts to fit these data to kinetic models using global fitting (Specfit™) were not successful. Therefore initial rates have been used, but even these were not very satisfactory, since even the first $5 - 10\%$ of the reactions exhibited some nonlinearity. Still, a rate of $d[Co^{III}]_{total}/dt \approx 6.6 \times 10^{-8}$ M s^{-1} was estimated for a reaction of 0.59 mM $Co^{III}Hbim +$ 46.4 mM H_2Q, which yields ~0.021 mM BQ in the first $5 - 10\%$ of the reaction (where $[Co^{III}]_{total}$ refers to the $Co^{III}Hbim + Co^{III}Hbim\text{--}H_2Q$ mixture). Analysis of the initial rate data over the first 15% of the reaction suggested that the kinetics might be second order in $[Co^{III}]_{total.}$ However, a control experiment in parallel with the initial rate experiment showed that a solution of 0.57 mM $Co^{III}Hbim$ decomposed significantly in the presence of 0.021 mM BQ. The initial rate of decomposition over the first 15% of the reaction, $d[Co^{III}]_{total}/dt \approx 1.4 \times 10^{-8}$ M s^{-1}, is ~20% of the initial rate quoted above for the reaction of 46.4 mM H_2Q. Due to these complications, further analyses of rates for the reaction of $Co^{III}Hbim + H_2Q$ were not pursued.

V. Marcus Cross Relation Analysis.

We have found that the Marcus cross relation[1,2] holds for many HAT reactions, including the iron analogs of reactions 4 and 5, $\mathbf{Fe^{II}H_2bim}$ + TEMPO or ${}^tBu_3ArO^{\bullet}$.[3,4,] The cross relation was developed for ET reactions and typically holds fairly well for Co(III)/Co(II) spin-forbidden ET reactions.[6] The cross relation cannot be tested directly for reactions 4 – 6 (main text) because the $\mathbf{Co^{III}Hbim/Co^{II}H_2bim}$ HAT self exchange rate constant is not directly measurable (a competing inner-sphere [ligand exchange] pathway is faster).[7] However, $k_{CoH/Co}$ can be estimated using the cross relation. This detailed discussion is a revision of the brief analysis of these cobalt reactions in the previous paper focused on direct measurements of self-exchange reactions.[7]

We have typically applied the cross relation in its simplest form, eq S2, using measured bimolecular rate constants.

$$k_{XH/Y} = \sqrt{k_{XH/X} k_{YH/Y} K_{XH/Y} f} \qquad (S2)$$

For the TEMPO reaction, $K_{XH/Y} = K_4 = (5.9 \pm 0.8) \times 10^{-3}$, $k_{TEMPOH/TEMPO} = 4.7$ M^{-1} s^{-1},[9] and $k_{XH/Y} = {}^1\!/_6 k_4 = (3.0 \pm 0.9) \times 10^{-5}$ M^{-1} s^{-1} (the factor of ${}^1\!/_6$ being the statistical correction for the six identical hydrogen atoms in $\mathbf{Co^{II}H_2bim}$). Inserting these values into equation S2, and determining f using an iterative procedure in Microsoft Excel (see below), gives the cobalt self-exchange rate $k_{CoH/Co(T)} = 4 \times 10^{-8}$ M^{-1} s^{-1} ($f = 0.91$). For the reaction with ${}^tBu_3ArO^{\bullet}$, $K_5 = 3 \times 10^5$, $k_{ArOH/ArO} = 20$ M^{-1} s^{-1},[10] and $k_{XH/Y} = {}^1\!/_6 k_{5H} = 28 \pm 4$ M^{-1} s^{-1} yield $k_{CoH/Co(ArO)} = 3 \times 10^{-4}$ M^{-1} s^{-1} ($f = 0.5$). The two derived values of the cobalt self-exchange rate constant differ by a factor of about 10^4. The kinetic complexity of the benzoquinone reaction precludes a similar Marcus analysis.

(1)   Marcus, R. A.; Sutin, N. *Biochim. Biophys. Acta* **1985**, *810*, 265–322.

(2)   Sutin, N. *Prog. Inorg. Chem.* **1983**, *30*, 441–499.

(3)   Mayer, J. M. *Acc. Chem. Res.* **2011**, *44*, 36–46.

(4)   Roth, J. P.; Yoder, J. C.; Won, T.-J.; Mayer, J. M. *Science*, **2001**, *294*, 2524–2526.

(5)   Mader, E. A.; Larsen, A. S.; Mayer, J. M. *J. Am. Chem. Soc.* **2004**, *126*, 8066-8067.

(6)   (a) Chou, M.; Creutz, C.; Sutin, N. *J. Am. Chem. Soc.* **1977**, *99*, 5615–5623.   (b) Gribble, J.; Wherland, S. *Inorg. Chem.* **1989**, *28*, 2859–2863.   (c) Doine, H.; Swaddle, T. W. *Inorg. Chem.* **1991,** *30*, 1858–1862.   (d) Grace, M. R.; Takagi, H.; Swaddle, T. W. *Inorg. Chem.* **1994**, *33*, 1915–1920. (e) Shalders, R. D.; Swaddle, T. W. *Inorg. Chem.* **1995**, *34*, 4815-4820.   (f) Wherland, S. *Coord. Chem. Rev.* **1993**, *123*, 169-199.

(7)   Yoder, J. C.; Roth, J. P.; Gussenhoven, E. M.; Larson, A. S.; Mayer, J. M. *J. Am. Chem. Soc.* **2003**, *125*, 2629–2640.

(8)   Mader, E. A.; Manner, V. W.; Markle, T. F.; Wu, A.; Franz, J. A.; Mayer, J. M. *J. Am. Chem. Soc.* **2009**, 131, 4335–4345.

(9)   (a) Wu, A.; Mader, E. A.; Datta, A.; Borden, W. T.; Mayer, J. M. *J. Am. Chem. Soc.* **2009**, *131*, 11985–11997. (b) Mader, E. A.; Larsen, A. S.; Mayer, J. M. *J. Am. Chem. Soc.* **2004**, *126*, 8066-7.

(10) Warren, J. J.; Mayer, J. M. *Proc. Nat. Acad. Sci. U.S.A.* **2010**, *107*, 5282–5287.

One origin of the discrepancy in the calculated self-exchange rate constants could be that the simple application of eq S2 ignores the involvement of precursor and successor complexes, such as are shown for the TEMPO reaction in eq 4 of the paper. We have typically ignored the formation of these complexes ("work terms" in the ET literature) because the energies are small and not available. In reaction 4, measurements show that the driving force for the actual unimolecular HAT step, **Co^{II}H$_2$bim**|TEMPO → **Co^{III}Hbim**|TEMPOH, $\Delta G_4°' = 0.3 \pm 0.9$ kcal mol^{-1}, is -2.7 ± 0.9 kcal mol^{-1} lower than the overall $\Delta G_4°$.[11]

The adiabatic Marcus Cross Relation including 'work terms' is given in equation S3, in which the rate constants are first-order rate constants for conversion of the precursor to successor complexes, and $K_{AH/B}$ is the equilibrium constant for AH|B → A|HB.[2]

$$k_{AH/B} = \left(\sqrt{k_{AH/A} k_{BH/B} K_{AH/B} f_{AH/B}} \right) \times W_{AH/B} \tag{S3}$$

Where $W_{AH/B}$ and $f_{AH/B}$ are defined by equations S4 and S5:

$$f_{AH/B} = \exp \left\{ \frac{[\ln K_{AH/B} + (w_P - w_S)/RT]^2}{4[\ln(k_{AH/A} k_{H/BB}/Z^2) + (w_{AH/A} + w_{BH/B})/RT]} \right\} \tag{S4}$$

$$W_{AH/B} = \exp \left[\frac{-(w_P + w_S - w_{AH/A} - w_{BH/B})}{2RT} \right] \tag{S5}$$

In these equations, $k_{AH/B}$ is the unimolecular rate constant of the cross reaction, $k_{AH/A}$ and $k_{BH/B}$ are the unimolecular self exchange rate constants for each reactant, $K_{AH/B}$ is the equilibrium constant for the bimolecular reaction, $w_{AH/A}$ and $w_{BH/B}$ are the work terms for the self exchange reactions, $w_P = \Delta G_P°$ is the work term to form the precursor complex, $w_S = \Delta G_S°$ is the work term to form the successor complex, Z the collision frequency is typically taken as 10^{11} M^{-1}s^{-1}, and R (the gas constant) $= 0.0019872$ kcal K^{-1} mol^{-1}.

For the reaction of **Co^{II}H$_2$bim** + TEMPO, these equations were solved using an iterative procedure in Excel, using the Goal Seek function and varying the value of $k_{AH/A}$ in order to make eq S6 true. From Scheme S1, the following values were used: $w_P = \Delta G_{4P}° \sim 0.27$ kcal mol^{-1} and $w_S = \Delta G_{4S}° = -2.44$ kcal mol^{-1}, obtained from $K_{4P} \sim 0.6$ M^{-1} and $K_{4S} = 61.3 \pm 0.8$ M^{-1}.[11] For the unimolecular rate constant, $k_{AH/B} = {}^1/_6 k_{4HAT} = k_4/6K_{4P} = 4.7 \times 10^{-5}$ s^{-1}, where $k_4 = (1.8 \pm 0.5) \times 10^{-4}$ M^{-1}s^{-1} ($k_{AH/B}$ is statistically corrected for the six H-atoms in **Co^{II}H$_2$bim**). For the TEMPO

(11) Mader, E. A.; Mayer, J. M. *Inorg. Chem.* **2010**, *49*, 3685–3687. This report defines reaction 4 in the opposite direction (from **Co^{III}(Hbim)** + TEMPOH) so the thermochemical values are of opposite sign and $\Delta G_{4P}°$ here corresponds to $\Delta G_S°$ in that paper, and $\Delta G_{4S}°$ here corresponds to $\Delta G_P°$.

self exchange reaction, assuming that the precursor and successor complexes have $K_{eq} \sim 1$ and that $w_{BH/B} \sim 0$ because both TEMPO and TEMPOH are neutral,[12] then the unimolecular self-exchange rate constant is $k_{BH/B} = k_{TEMPO} = 4.7$ M^{-1}s^{-1} ~ 4.7 s^{-1}. The work term for the self exchange reaction, **Co^{II}H$_2$bim + Co^{III}Hbim**, is modeled as the purely electrostatic value, $w_{AH/A}$ $= w_{Co} \sim +3.9$ kcal mol^{-1}.[13] The equilibrium constant for the bimolecular reaction is $K_{AH/B} = K_4 =$ 5.9×10^{-3}. Solving eq S6 using these values, including the full equations for both $W_{AH/B}$ and $f_{AH/B}$, gives $k_{AH/A} = k'_{CoH/Co(T)} = 3 \times 10^{-12}$ s^{-1}. Note that this first-order rate constant cannot be directly compared with the bimolecular $k_{CoH/Co(T)} = 4 \times 10^{-8}$ M^{-1} s^{-1} given in the main text.

$$1 = \frac{\left(\sqrt{k_{AH/A}k_{BH/B}K_{AH/B}f_{AH/B}}\right) \times W_{AH/B}}{k_{AH/B}} \qquad (S6)$$

Scheme S1.

---
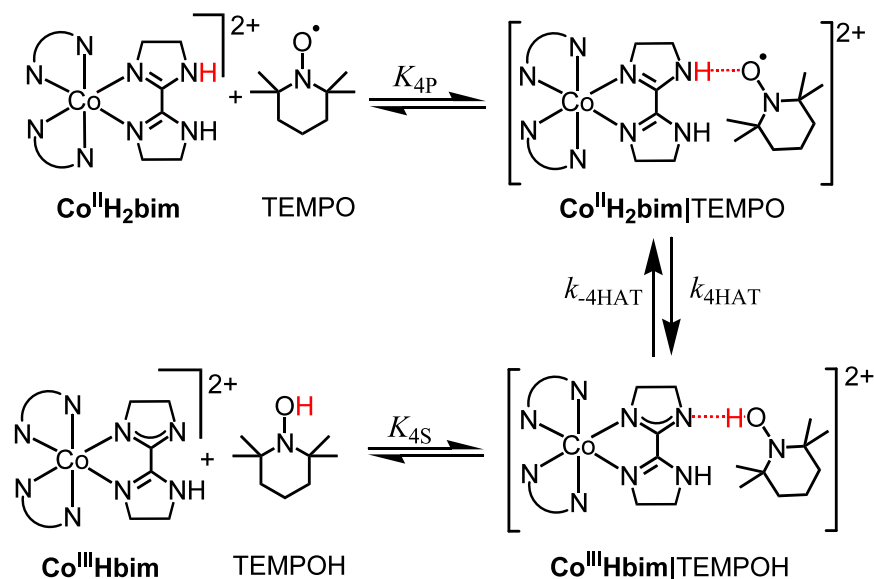
(12) Eberson, L. *Electron Transfer Reactions in Organic Chemistry*, Springer-Verlag: Berlin, Germany, 1987, p. 27–28.

(13) (a) From reference 12, $w_{AH/A} = Z_1Z_2e^2f / r_{12}D$, where $D = 35$ (the dielectric constant for MeCN), $Z_1 =$ 2 and $Z_2 = 2$ (the charges for **Co^{II}H$_2$bim** and **Co^{III}Hbim**), $e^2 = 331.2$ Å kcal mol^{-1},[12] $f = 1$ (factor defining ionic strength), and $r_{12} = 9.64$ Å (the collision distance in the self-exchange reaction between **Co^{II}H$_2$bim** and **Co^{III}Hbim**, estimated from the crystal structures for **Co^{II}H$_2$bim** and **Co^{III}H$_2$bim**[13b]). (b) The structure of **Co^{II}H$_2$bim** has an average distance of 4.85 Å between Co and each N–H hydrogen, and the structure of **Co^{III}H$_2$bim** has an average distance of 4.79 Å between Co and each N–H hydrogen (there is no structure for **Co^{III}Hbim**).[13c] Added together, they give an estimate for r_{12}. (c) Yoder, J. C.; Roth, J. P.; Gussenhoven, E. M.; Larsen, A. S.; Mayer, J. M. *J. Am. Chem. Soc.* **2003**, *125*, 2629–2640.

In the reaction of $\mathbf{Co^{II}H_2bim}$ + ${}^t\mathbf{Bu_3ArO^\bullet}$, $W_{AH/B}$ and $f_{AH/B}$ were included when solving for eq S6, but with the assumption that $w_P \sim w_S \sim 0$, since no precursor or successor complexes could be experimentally observed. The bimolecular equilibrium constant, $K_{AH/B} = K_5 = 3 \times 10^5$. The unimolecular rate constants can be estimated (assuming that $K_{eq} \sim 1$ M^{-1} for the formation of precursor complexes in each case), giving $k_{BH/B} = k_{ArO} = 20$ M^{-1} s$^{-1} \sim 20$ s^{-1} and $k_{AH/B} = {}^1\!/_6 k_{5H} = 28 \pm 4$ M^{-1} s$^{-1} \sim 28$ s^{-1}. Using $w_{Co} \sim 3.9$ kcal mol^{-1} (as above) gives $k_{AH/A} = k'_{CoH/Co(ArO)} = 3 \times 10^{-7}$ s^{-1}. This is 10^5 larger than the TEMPO value. Since including precursor and successor complexes makes discrepancy in self-exchange rate constants larger, the poor agreement with the cross relation likely lies elsewhere. Potentially, the discrepancy is due the ${}^t\mathrm{Bu_3ArO^\bullet}$ reaction not occurring by HAT, as described in the main paper.

It should be noted that the cross relation is more accurate at predicting cross rate constants than self-exchange ones. Using the geometric mean of the bimolecular self-exchange rate constants for $\mathbf{Co^{II}H_2bim}$ above, 3×10^{-6} M^{-1} s^{-1}, the two cross rates are predicted to within about an order of magnitude. This is fairly typical agreement for application of the cross relation to HAT.[3,11] This crude estimate of the $\mathbf{Co^{II}H_2bim}$ HAT self-exchange rate constant is *10^9 times* slower than that for the analogous iron reaction, $k_{FeH/Fe} = (5.8 \pm 0.6) \times 10^3$ M^{-1} s^{-1}.[14] The outer-sphere *electron transfer* self-exchange rate constant for $\mathbf{Co^{II}H_2bim}$ + $\mathbf{Co^{III}H_2bim}$ is estimated to be in the same range, $\sim 10^{-6}$ M^{-1} s^{-1}.[7] Such a slow ET self-exchange rate is common for cobalt complexes. With ethylenediamine ligands, for instance, electron exchange between low-spin $Co(en)_3{}^{3+}$ and high-spin $Co(en)_3{}^{2+}$ has $k_{s.e.} = 3.4 \times 10^{-5}$ M^{-1} s^{-1}.[15] Still, a wide range of ET self-exchange rate constants are known for Co complexes from *ca.* 10^{-12} M^{-1} s^{-1} for the $Co(OH_2)_6{}^{3+/2+}$ couple,[6] to $\sim 10^1$ M^{-1} s^{-1} for $Co(bpy)_3{}^{3+/2+}$ and the sepulchrate complex, $Co(sep)^{3+/2+}$ (sep = 1,3,6,8,10,13,16,19-octaazabicyclo[6.6.6]eicosane;[16] both $Co(bpy)_3{}^{2+}$ and $Co(sep)^{2+}$ are high spin).[6,15a]

(14) Roth, J. P.; Lovell, S.; Mayer, J. M. *J. Am. Chem. Soc.* **2000**, *122*, 5486–5498.

(15) (a) Endicott, J. F.; Kumar, K.; Ramasami, T.; and Rotzinger, F. P. *Prog. Inorg. Chem.* **1983**, *30*, 141–187. (b) Dwyer, F. P.; Sargeson, A. M. *J. Phys. Chem.* **1961**, *65*, 1892–1894.

(16) Creaser, I. I.; Geue, R. J.; Harrowfield, J. M.; Herlt, A. J.; Sargeson, A. M.; Snow, M. R.; Springborg, J. *J. Am. Chem. Soc.* **1982**, *104*, 6016–6025.

Table S3. Values used for Marcus Treatment in reactions of $\mathbf{Co^{II}H_2bim}$ + TEMPO/^{t}Bu$_3$ArO$^\bullet$.

$\mathbf{Co^{II}H_2bim}$ + X$^\bullet$	TEMPO	^{t}Bu$_3$ArO$^\bullet$
$k_{AH/B}$	4.7×10^{-5} s^{-1}	28 s^{-1}
$k_{BH/B}$	4.7 s^{-1}	20 s^{-1}
$K_{AH/B}$	5.9×10^{-3}	3×10^5
w_P	0.27 kcal mol^{-1}	0 kcal mol^{-1}
w_S	-2.44 kcal mol^{-1}	0 kcal mol^{-1}
$w_{AH/A}$	3.9 kcal mol^{-1}	3.9 kcal mol^{-1}
$w_{BH/B}$	0 kcal mol^{-1}	0 kcal mol^{-1}
ca. $\mathbf{k_{AH/A}}$	$\mathbf{3 \times 10^{-12}}$ **s^{-1}**	$\mathbf{3 \times 10^{-7}}$ **s^{-1}**

VI. Estimation of the energy of the ^2E_g state for $[Co^{II}(H_2bim)_3]^{2+}$.

The optical spectrum of $[Co^{II}(H_2bim)_3]^{2+}$ in MeCN (Figure S3) has a broad band at $\lambda_{max} = 1035$ nm = 9,660 cm^{-1} ($\varepsilon = 11$ L mol^{-1} cm^{-1}) and a sharper band at 485 nm = 20,600 cm^{-1} ($\varepsilon = 46$ L mol^{-1} cm^{-1}). The latter band is in agreement with a prior report.[13c]
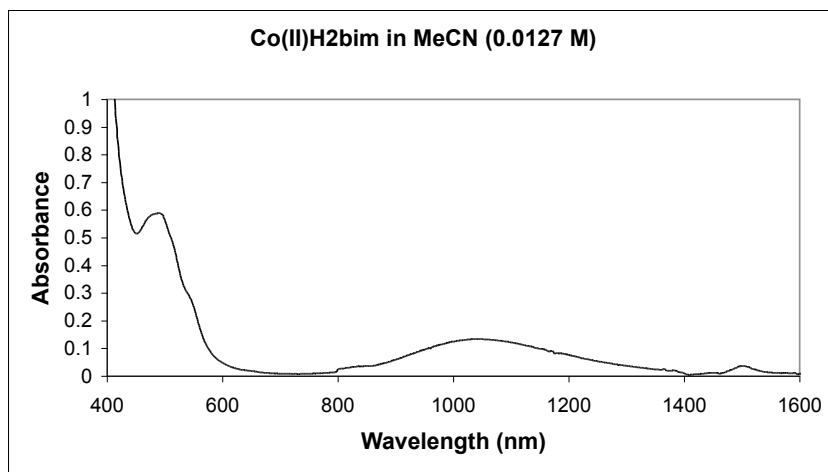

Figure S3. Optical spectrum of **CoH$_2$bim** in MeCN.

Based on analyses of related spectra,[17,18,19] it is very likely that the 485 nm band is due to $^4T_{1g}(F) \rightarrow {}^4T_{1g}(P)$ transition and the 1035 nm band is due to $^4T_{1g}(F) \rightarrow {}^4T_{2g}$ transition. The energy of the latter transition is close to but a bit below Δ_o. From these values, the ratio:

$$E[^4T_{1g}(F) \rightarrow {}^4T_{1g}(P)]/E[^4T_{1g}(F) \rightarrow {}^4T_{2g}] = 2.13$$

From the d^7 Tanabe-Sugano diagram (Figure S5), that ratio occurs at about $\Delta_o/B = 15$. At $\Delta_o/B = 15$, the energy of the $^4T_{2g}$ state is ~14 B, so 14B = 9,660 cm^{-1}, or B = 690 cm^{-1}. Similarly, the $^4T_{1g}(P)$ state has energy 30 B, which gives 30B = 20,600 cm^{-1} or B = 687 cm^{-1}. The good agreement between these two values supports this analysis. The B value for $[Co(NH_3)_6]^{2+}$ is higher, 885 cm^{-1},[18] consistent with the greater delocalization in the H$_2$bim ligand than in ammonia.

(17) Li, W.-K.; Zhou, G.-D.; Mak, T. *Advanced Structural Inorganic Chemistry* Oxford University Press, Oxford, 2008, p. 274.
(18) Figgis, B. N.; Mitchman, M. A. *Ligand Field Theory and Its Applications* Wiley-VCH, New York, 2000, pp. 208-9, 220.
(19) (a) Krivokapic, I.; Zerara, M.; Dakua, M. L.; Vargas, A.; Enachescu, C.; Ambrusc, C.; Tregenna-Piggott, P.; Amstutz, N.; Krausz, E.; Hauser, A. *Coord. Chem. Rev.* **2007**, *251*, 364–378. (b) Beattie, J. K.; Binstead, R. A.; Kelso, M. T.; Favero, P.; Dewey, T. G.; Turner, D. H. *Inorg. Chim. Acta* **1995**, *235*, 245-251. (c) Beattie, J. K. *Adv. Inorg. Chem.* **1988**, *32*, 1–49.

With these parameters, the energy of the $^2E_{2g}$ state is 6.67 B = 4,600 cm^{-1}, or 13 kcal mol^{-1}. A weak band in the near IR spectrum at 2180 nm (4590 cm^{-1}, Figure S4) could be due to this transition.
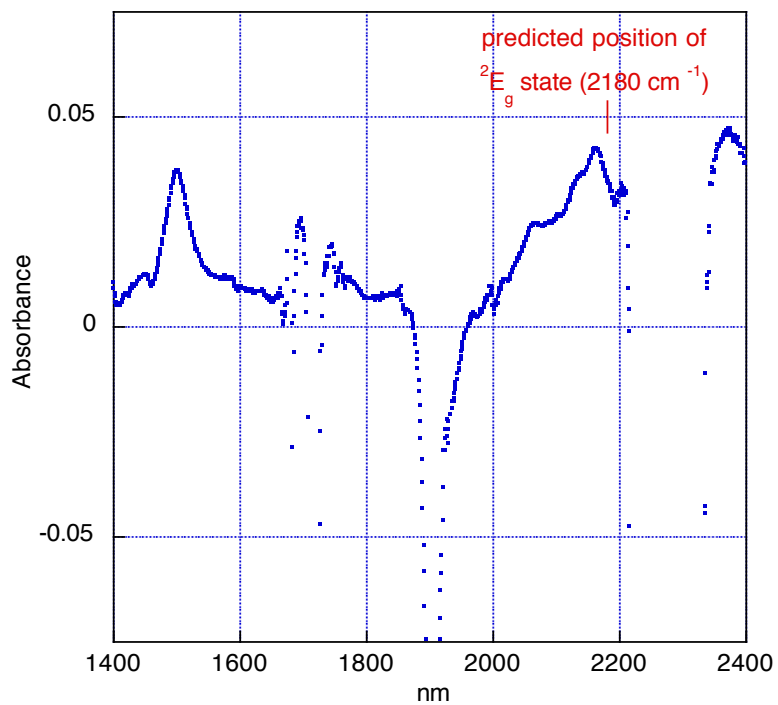

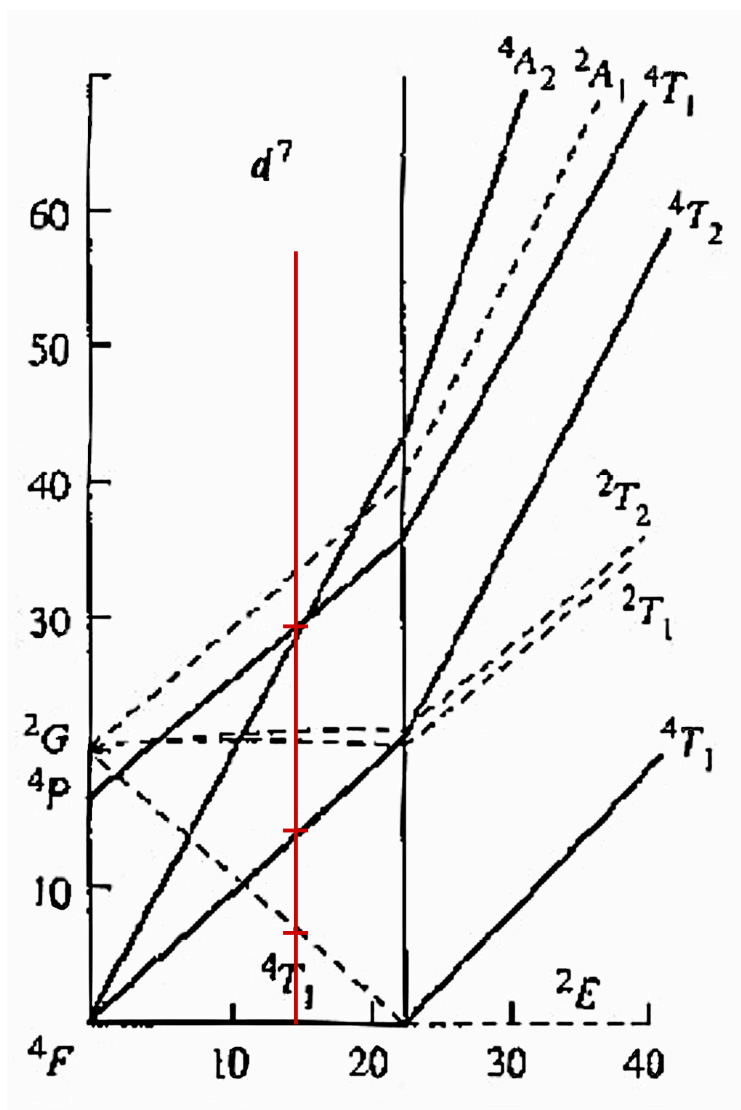**Figure S4.** Near-IR Spectrum of **CoH$_2$bim** in MeCN.

Figure S5. d^7 Tanabe-Sugano diagram from:
http://wwwchem.uwimona.edu.jm/courses/Tanabe-Sugano/TanSugd7hs.html

VII. Detailed Experimental Methods.

General Considerations. All manipulations were carried out under nitrogen using glovebox/vacuum line techniques. ^{1}H NMR spectra were obtained on Bruker Avance spectrometers (Avance-500, DRX-499, and Avance-300), and are reported as (chemical shift δ, assignment, number of protons). All NMR integration errors are estimated as ±10%. UV-visible spectra were obtained with a Hewlett-Packard 8453 diode-array spectrophotometer. Air-sensitive samples were prepared in a glovebox in quartz cuvettes attached to Teflon-stoppered valves and topped with 14/20 ground glass joints ('Kontes cuvettes'). In one case, an injectable screw-capped cuvette was used with a silicone/PFTE septum (Spectrocell). Rapid kinetic measurements were taken using an OLIS RSM-1000 stopped flow instrument which has a rapid scanning monochromator and a UV-Vis detector.

Materials. Unless otherwise noted, all solvents were purchased from Fisher Scientific or EMD Chemicals. Anhydrous acetonitrile (MeCN; <10 ppm H_2O) was purchased from Honeywell Burdick & Jackson, sparged with argon, and plumbed from a steel keg directly into a glovebox. Deuterated CD_3CN was purchased from Cambridge Isotope Laboratories, dried over CaH_2, vacuum transferred to P_2O_5, then vacuum transferred to fresh CaH_2 and finally into an empty vessel. All reagents were purchased by Aldrich and used as received except for **H_2Q** and **BQ**. **H_2Q** was recrystallized 2-3 times in acetone or ethanol and dried under vacuum. **D_2Q** was prepared by recrystallizing **H_2Q** from D_2O/CD_3OD. **BQ** was recrystallized once in ethanol and then sublimed 1-2 times at room temperature under static vacuum. $[Cp^*_2Fe]PF_6$[20] and $^tBu_3ArO^{\bullet}$[21] were prepared according to literature procedures. Cobalt(II) tris[2,2'-bi-2-imidazoline][perchlorate] ($[Co^{II}(H_2bim)_3][ClO_4]_2$, **$Co^{II}H_2bim$**) and $[Co^{III}(H_2bim)_3][ClO_4]_3$ (**$Co^{III}H_2bim$**); and $[Co^{III}(H_2bim)_2(Hbim)][ClO_4]_2$ (**$Co^{III}Hbim$**) were synthesized and characterized following literature procedures.[22] *Caution: perchlorate salts are explosive and should be handled with care and in small quantities. They should not be heated when dry or subjected to friction or shock, such as scratching with a non-Teflon-coated spatula.*

K_{eq} for $Co^{II}H_2bim$ + $[Cp^*_2Fe]PF_6$ $\rightleftarrows$ $Co^{III}H_2bim$ + Cp^*_2Fe. Four Kontes cuvettes were each charged with 2 mL of a 1.32 mM MeCN solution of $[Cp^*_2Fe]PF_6$ (6.2 mg in 10 mL). **$Co^{II}H_2bim$** was added as a solid to three of the four cuvettes to form 1.12, 1.93, and 3.35 mM solutions.

(20) Duggan, D. M.; Hendrickson, D. N. *Inorg. Chem.* **1975**, *14*, 955–970.

(21) Manner, V. W.; Markle, T. F.; Freudenthal, J. H.; Roth, J. P.; Mayer, J. M. *Chem. Commun.* **2008**, 256–258.

(22) Yoder, J. C.; Roth, J. P.; Gussenhoven, E. M.; Larson, A. S.; Mayer, J. M. *J. Am. Chem. Soc.* **2003**, *125*, 2629–2640.

Spectra of the three reaction cuvettes showed a slow drop in absorbance at 780 nm (λ_{max} for $Cp^*_2Fe^+$), over *ca.* 4,000 sec. Good mass balance was observed, with a reasonable isosbestic point at $\lambda = 593 \pm 1$ nm. The final, constant absorbance gave the concentration of $[Cp^*_2Fe]PF_6$ at equilibrium, using $\varepsilon_{780} = 600$ M^{-1} cm^{-1} (no other species absorb at 780 nm). Assuming mass balance, $[Cp^*_2Fe]_{eq} = [Cp^*_2FePF_6]_{initial} - [Cp^*_2FePF_6]_{eq}$, $[\mathbf{Co^{III}H_2bim}]_{eq} = [Cp^*_2Fe]_{eq}$, and $[\mathbf{Co^{II}H_2bim}]_{eq} = [\mathbf{Co^{II}H_2bim}]_{initial} - [Cp^*_2Fe]_{eq}$. As a confirmation of mass balance, for each experiment the equilibrium absorbance at 510 nm (the λ_{max} for $\mathbf{Co^{III}H_2bim}$ and where all four species absorb) was within 6% of the value predicted based on K_3 and the extinction coefficients for all species [$\mathbf{Co^{III}H_2bim}$ + $[Cp^*_2Fe]PF_6$ ($\varepsilon_{[Cp*2Fe]PF6,510} = 90$ M^{-1} s^{-1}) + $\mathbf{Co^{II}H_2bim}$ ($\varepsilon_{CoII,510} = 50$ M^{-1} s^{-1}) + Cp^*_2Fe ($\varepsilon_{Cp*2Fe,510} = 15$ M^{-1} s^{-1})]. The derived concentrations give the constant $K_3 = [\mathbf{Co^{III}H_2bim}][Cp^*_2Fe]/[\mathbf{Co^{II}H_2bim}][Cp^*_2Fe^+] = 0.090 \pm 0.032$ and $E = (RT/F)\ln(K_3) = -0.062 \pm 0.011$ V. Since $E_{1/2}([Cp^*_2Fe]PF_6) = -0.59$ V *vs.* $Cp_2Fe^{+/0}$ in MeCN,[23] $E_{1/2}(\mathbf{Co^{III}H_2bim}) = -0.53 \pm 0.02$ V *vs.* $Cp_2Fe^{+/0}$ in MeCN. No supporting electrolyte was used for these measurements or for the kinetics below; the pK_a of $\mathbf{Co^{III}H_2bim}$ was found to be the same in the presence and absence of NBu_4PF_6.[24]

$\mathbf{Co^{II}H_2bim}$ + $^t\mathbf{Bu_3ArO^{\bullet}}$ by ^{1}H NMR Spectroscopy. Two J. Young NMR tubes were charged with 400 μL of a solution of $\mathbf{Co^{II}H_2bim}$ (11.5 mM, 11.6 mg in 1.5 mL CD_3CN), and solid $^tBu_3ArO^{\bullet}$ (0.8 equiv, 9.6 mM, 1.0 mg) was added to one of the tubes. ^{1}H NMR spectra were recorded within 1 h, and integrations relative to HMDS were determined using Mestre-C^{TM} for $\mathbf{Co^{II}H_2bim}$ (δ21-22 ppm), $\mathbf{Co^{III}Hbim}$ (δ2.5-5 ppm), and $^tBu_3ArOH$ (δ7-7.5 ppm, δ1.2-1.6 ppm). Versus the integration of $\mathbf{Co^{II}H_2bim}$ in the control solution, the yield of $\mathbf{Co^{III}Hbim}$ was 83% and $^tBu_3ArOH$ was 80%, as expected for 0.8 equiv $^tBu_3ArO^{\cdot}$, with 17% $\mathbf{Co^{II}H_2bim}$ remaining.

$\mathbf{Co^{II}H_2bim}$ + $^t\mathbf{Bu_3ArO^{\bullet}}$: Stopped-Flow Kinetics. In the glovebox, two syringes were loaded with MeCN solutions of $\mathbf{Co^{II}H_2bim}$ (2.72 mM) and $^tBu_3ArO^{\bullet}$ (1.64 – 4.21 mM), respectively. The syringes were removed from the glovebox and immediately attached to the stopped-flow. For runs at higher temperature, the system was thermally equilibrated for 10-15 min before data acquisition. At least six kinetic runs were performed per set (all concentrations become diluted by half in the stopped-flow). The data were fit to mixed second-order kinetics using the OLIS SVD global fitting software. The average rate constant for each set of runs was plotted *vs.* [$^tBu_3ArO^{\bullet}$] using KaleidaGraph software, weighting each rate constant with 2× its standard deviation and fitting to a line of zero slope, to determine an overall rate constant. The kinetic

(23) Connelly, N. G.; Geiger, W. E. *Chem. Rev.* **1996**, *96*, 877-910.

(24) Roth, J. P. *Intrinsic and Thermodynamic Influences on Hydrogen Atom Transfer Reactions Involving Transition Metal Complexes*, Ph.D. Thesis, University of Washington, Seattle, WA, 2000, pp. 128–129.

isotope effect was determined following a version of the procedure above. A solution of **Co^{II}H$_2$bim** (1.36 mM) was prepared. A 15 mL portion was set aside, a 25 mL portion was mixed with 850 μL CD$_3$OD (to give 1.31 mM **Co^{II}D$_2$bim** and 0.81 M CD$_3$OD), and another 10 mL was mixed with 340 μL CH$_3$OH (to form 1.31 mM **Co^{II}H$_2$bim** and 0.81 M CH$_3$OH). Each of these solutions was reacted with 1.64 – 4.21 mM solutions of ^{t}Bu$_3$ArO$^{\bullet}$ in the stopped-flow, at least five kinetic runs were performed per set of solutions, and the data was analyzed as above.

K_{eq} for Co^{III}Hbim + ½ H$_2$Q $\rightleftharpoons$ Co^{II}H$_2$bim + ½ BQ by ^{1}H NMR Spectroscopy. Four J. Young NMR tubes were charged with 500 μL of 4 mM **Co^{III}Hbim** solution containing HMDS, and solid **H$_2$Q** was added to four of the five tubes to give 50.9, 74.5, and 105.3 mM solutions. ^{1}H NMR spectra were obtained at intervals from 40 min – 44 h, monitoring the integrals of **Co^{II}H$_2$bim** (δ21-22 ppm), **Co^{III}Hbim** (δ2.5-5 ppm), and {**H$_2$Q + BQ**} (δ 6 – 7 ppm). The spectra stopped changing after 20 hours, and at least three spectra were obtained per tube after that time. Because of the large excesses of **H$_2$Q**, a separate peak for **BQ** could not be integrated. The final total cobalt integration, **Co^{II}H$_2$bim + Co^{III}Hbim**, was 24 ± 14% lower than the tube with only **Co^{III}Hbim** (which did not decay), indicating some decomposition. Despite this decomposition, to obtain estimates of the equilibrium constant K_6 mass balance was assumed, that [**BQ**] = ½[**Co^{II}H$_2$bim**] and that [**H$_2$Q**] = [**H$_2$Q + BQ**]$_{total}$ – ½[**Co^{II}H$_2$bim**]. The NMR integrations then give values of K_6 = [**Co^{II}H$_2$bim**][**H$_2$Q**]$^{0.5}$/[**Co^{III}Hbim**][**BQ**]$^{0.5}$ that range from 2.0 to 2.9 with an average value of K_6 = 2.4 ± 0.8.

K_{eq} for Co^{III}Hbim + H$_2$Q $\rightleftharpoons$ Co^{III}Hbim--H$_2$Q. Kontes cuvettes were charged with 2 mL of solutions of **Co^{III}Hbim** in MeCN (0.28 – 0.76 mM) and their Teflon stopcocks closed. Varying amounts of **H$_2$Q** were loaded above the closed valves (in some cases, MeCN was added to dissolve the solid **H$_2$Q**), and above those solutions the 14/20 joint was sealed with a rubber septum. An initial UV-vis spectrum (with absorbance A$_i$ at 586 nm) was taken of the **Co^{III}Hbim** solution, and then the Teflon valve was opened to allow the **H$_2$Q** into the solution (forming 5.90 – 407 mM **H$_2$Q**) while the septum maintained the N$_2$ atmosphere. After vigorous mixing, a second spectrum (with absorbance A$_2$ at 586 nm) was taken at ≤ 2 minutes of reaction, and then additional spectra were obtained over ~ 8 h (to monitor the kinetics). At [**H$_2$Q**] = 346 – 407 mM, the A$_2$ absorbance remained constant within 4%, indicating quantitative formation of the **Co^{III}Hbim--H$_2$Q** hydrogen-bonded complex, and giving $\varepsilon_{CoIII-H2Q}$(586 nm) ~ 350 M^{-1} cm^{-1}. Assuming mass balance, [**Co^{III}Hbim--H$_2$Q**]$_{eq}$ = (A$_2$ – A$_i$)/($\varepsilon_{CoIII-H2Q}$ – $\varepsilon_{CoIIIHbim}$), and [**Co^{III}Hbim**]$_{eq}$ = [**Co^{III}Hbim**]$_i$ – [**Co^{III}Hbim--H$_2$Q**]$_{eq}$. Being in large excess, [**H$_2$Q**]$_{eq}$ ≈ [**H$_2$Q**]$_i$. The plot of [**Co^{III}Hbim--H$_2$Q**]$_{eq}$ *vs.* ([**Co^{III}Hbim**]$_{eq}$[**H$_2$Q**]$_{eq}$) (Figure S1) has a slope of 14 ± 2 M^{-1} with a nonzero intercept (8 × 10^{-5} M) which may indicate some decomposition or reaction on the timescale of the experiment. Forcing the plot through (0,0) gives a slope of 21 M^{-1}, so K_{6S} was taken to be 14 ± 7 M^{-1}.

Co^{III}Hbim + H$_2$Q UV-Vis Kinetics. In the experiment above, optical spectra were collected over ~ 8 h. The absorbance at 586 nm was analyzed over the first 15% of reaction, until $A_{15} = A_i - 0.15(A_i - A_f)$ at time t_{15}, where A_f is the final absorbance for that particular reaction. The ε_{586} of the **Co^{III}Hbim + Co^{III}Hbim--H$_2$Q** mixture was calculated from the first kinetics scan (A_i), and is assumed to be constant during the initial 15% of the reaction due to the large excess of **H$_2$Q**. $d[Co^{III}]_{total}/dt = (A_i - A_{15})/t_{15}\varepsilon_{CoIII} = 6.6 \times 10^{-8}$ M s^{-1}. The deuterium transfer reaction was done and analyzed following the same procedures, using **Co^{III}Dbim** and **D$_2$Q**. **Co^{III}Dbim** was generated by adding 250 μL of CD$_3$OD to 10 mL of a MeCN solution of **Co^{III}Hbim** in a Kontes cuvette, followed by removal of the solvent on the vacuum line; fresh MeCN was added to prepare the solutions for kinetic studies.

VIII. Computational Studies.

Co^{II}H$_2$bim   TEMPO   **Co^{III}Hbim**   TEMPOH
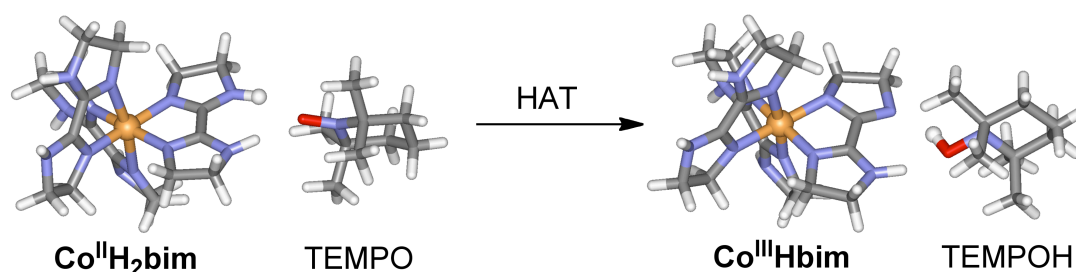
Figure S6. Calculated reactant and product complexes.

OPBE/BSI total energies and (zero-point energies) in Hartree,
Atomic Number Z, and x, y, z Cartesian Coordinates in Angstrom.

H atom
-0.501613567 (0.000000)
 1 0.000000 0.000000 0.000000

TEMPOH Hydroxylamine
-484.0983646 (0.272049)
 6 -1.244113 1.426718 -0.464369
 6 -1.290883 -0.051488 -0.025580
 6 1.290883 -0.051486 -0.025579
 6 1.244110 1.426719 -0.464370
 6 -0.000002 2.163022 0.017433
 1 -1.268044 1.462634 -1.565411
 1 -2.160186 1.923493 -0.110272
 1 2.160183 1.923496 -0.110274
 1 1.268040 1.462635 -1.565411
 1 -0.000002 2.256221 1.113702
 1 -0.000003 3.192502 -0.374244
 6 1.662093 -0.184613 1.466140
 1 1.519511 -1.219321 1.799653

 1 2.720691 0.074493 1.611477
 1 1.074971 0.470720 2.117901
 6 2.381283 -0.762296 -0.849763
 1 3.346811 -0.251668 -0.728020
 1 2.508016 -1.802900 -0.524918
 1 2.119688 -0.756961 -1.917083
 6 -1.662094 -0.184616 1.466139
 1 -2.720696 0.074476 1.611476
 1 -1.519499 -1.219321 1.799656
 1 -1.074982 0.470728 2.117898
 6 -2.381282 -0.762300 -0.849764
 1 -2.508016 -1.802903 -0.524917
 1 -3.346811 -0.251672 -0.728022
 1 -2.119686 -0.756968 -1.917083
 7 0.000001 -0.664709 -0.429110
 8 0.000004 -2.026202 0.013388
 1 0.000009 -2.505074 -0.831162

TEMPO nitroxyl radical
-483.49806808 (0.260224)
 6 1.403666 0.468638 1.239500
 6 -0.068537 0.027328 1.328025
 6 -0.068537 0.027328 -1.328025
 6 1.403666 0.468638 -1.239500
 6 2.126525 -0.041541 0.000000
 1 1.443542 1.570008 1.235418
 1 1.913643 0.143207 2.158800
 1 1.913643 0.143207 -2.158800
 1 1.443542 1.570008 -1.235418
 1 2.187690 -1.140082 0.000000
 1 3.165812 0.321993 0.000000
 6 -0.196064 -1.432785 -1.804325
 1 -1.245423 -1.746435 -1.742097
 1 0.131916 -1.519506 -2.849699
 1 0.407416 -2.124482 -1.204453
 6 -0.815088 0.939950 -2.313040
 1 -0.336857 0.888137 -3.300754
 1 -1.862188 0.633469 -2.408481
 1 -0.791934 1.983563 -1.971178
 6 -0.196064 -1.432785 1.804325
 1 0.131916 -1.519506 2.849699
 1 -1.245423 -1.746435 1.742097
 1 0.407416 -2.124482 1.204453
 6 -0.815088 0.939950 2.313040
 1 -1.862188 0.633469 2.408481
 1 -0.336857 0.888137 3.300754
 1 -0.791934 1.983563 1.971178
 7 -0.746762 0.171710 0.000000
 8 -2.011658 0.021486 0.000000

Co(H₂bim)₃²⁺ Quartet
-1506.1821146 (0.512188)
27 -0.005274 -0.005470 -0.005257
 6 -2.215828 -1.873279 -0.601033
 6 -1.531692 -2.476826 0.552962
 7 -0.542946 -1.815410 1.086179
 7 -1.695305 -0.796471 -1.120067
 7 -1.314683 1.344002 1.089299
 6 -1.385137 2.545842 0.588567
 6 -0.514000 2.862579 -0.553333
 7 0.169645 1.886897 -1.081722
 7 1.547075 -1.104645 -1.064526
 6 2.751116 -0.951656 -0.587739
 6 2.903443 -0.105333 0.604967
 7 1.830073 0.465716 1.075968
 7 4.072627 0.202964 1.224303
 1 4.857948 -0.438013 1.219329
 7 3.737492 -1.653245 -1.203732
 1 4.699846 -1.335092 -1.191339
 7 -1.867148 -3.650586 1.146773
 1 -2.311093 -4.397516 0.624699
 7 -2.227426 3.411338 1.207724
 1 -2.646776 4.188049 0.709384
 7 -0.389797 4.079785 -1.142305

 1 -0.531594 4.935196 -0.617156
 6 0.917518 2.460970 -2.204933
 1 1.973741 2.166980 -2.156131
 1 0.507262 2.062416 -3.146219
 6 0.715996 3.994324 -2.101937
 1 1.606265 4.511324 -1.710566
 1 0.438067 4.454468 -3.058310
 6 -2.236135 1.312021 2.229952
 1 -2.883360 0.427155 2.181366
 1 -1.649506 1.239685 3.159277
 6 -3.030051 2.641235 2.163064
 1 -4.054045 2.502763 1.781672
 1 -3.085092 3.155928 3.130351
 6 -0.817925 -3.969001 2.120561
 1 -1.255949 -4.284578 3.075671
 1 -0.177104 -4.781819 1.744284
 6 -0.065738 -2.616844 2.217880
 6 1.657274 -2.059556 -2.172033
 1 1.102242 -1.704269 -3.049251
 1 1.209417 -3.016572 -1.860062
 6 3.174397 -2.204715 -2.440579
 1 3.504037 -1.614597 -3.310710
 1 3.489195 -3.245616 -2.583593
 6 2.268143 1.324849 2.180546
 1 2.191536 2.376698 1.861896
 1 1.619174 1.195667 3.055778
 6 3.736647 0.922660 2.457327
 1 4.400007 1.784384 2.600245
 6 -3.776155 -1.362527 -2.180693
 1 -4.025075 -1.830568 -3.141171
 1 -4.670281 -0.841792 -1.803195
 1 -4.006350 -2.911684 -0.700056
 6 -2.538540 -0.434117 -2.264142
 1 -2.801568 0.630741 -2.229836
 1 -1.970465 -0.603299 -3.192380
 7 -3.322420 -2.367066 -1.213294
 1 1.024674 -2.733656 2.174570
 1 -0.304426 -2.088655 3.154382
 1 3.831359 0.257233 3.330395

Co(H₂bim)₃²⁺ Doublet
-1506.1692234 (0.51365)
27 -0.013515 0.064343 0.013160
 6 -2.273589 -1.488567 0.765853
 6 -2.863396 -0.780504 -0.379426
 7 -2.073899 0.010592 -1.044982
 7 -1.047949 -1.178090 1.111719
 7 0.754779 -1.419324 -1.012620
 6 1.946762 -1.867749 -0.712250
 6 2.686505 -1.210454 0.371964
 7 2.043490 -0.332067 1.081721
 7 -0.509911 1.630664 1.055333
 6 -0.111359 2.785857 0.582519
 6 0.628623 2.685053 -0.665897
 7 0.783882 1.455204 -1.092401
 7 1.236645 3.651226 -1.398033

1 0.868331 4.595903 -1.420313
7 -0.506028 3.881945 1.277024
1 0.044119 4.733794 1.262604
7 -4.134340 -0.920518 -0.848751
1 -4.906700 -1.179959 -0.246800
7 2.405148 -2.882798 -1.487436
1 3.080891 -3.544702 -1.122122
7 3.970363 -1.491513 0.736814
1 4.649896 -1.794012 0.047270
6 2.986273 0.122798 2.109338
1 2.996224 1.219412 2.168237
1 2.650355 -0.253504 3.089140
6 4.363194 -0.471865 1.717624
1 5.025717 0.275949 1.253268
1 4.891235 -0.927487 2.564432
6 0.264952 -2.212481 -2.146262
1 -0.756754 -2.563564 -1.963716
1 0.242535 -1.579458 -3.046038
6 1.279474 -3.371728 -2.290030
1 0.893444 -4.316352 -1.875357
1 1.585127 -3.545847 -3.329010
6 -4.335769 0.119663 -1.863786
1 -4.842494 -0.289225 -2.746789
1 -4.946405 0.942714 -1.459026
6 -2.875119 0.553362 -2.146776
6 -1.315412 1.910094 2.247119
1 -1.035122 1.250047 3.076133
1 -2.376058 1.731087 2.012124
6 -1.047616 3.402187 2.555510
1 -0.305152 3.530212 3.359341
1 -1.956752 3.952826 2.825370
6 1.630374 1.521434 -2.287415
1 2.632780 1.140295 -2.038589
1 1.224039 0.902993 -3.095778
6 1.670649 3.023825 -2.653175
1 2.672687 3.368111 -2.935922
6 -1.981549 -2.753717 2.643461
1 -2.399374 -2.287729 3.550996
1 -1.881492 -3.832028 2.817675
1 -3.830395 -2.668546 1.513074
6 -0.661113 -2.087300 2.197518
1 0.053681 -2.826646 1.805572
1 -0.165956 -1.541754 3.008473
7 -2.836239 -2.484236 1.488296
1 -2.760125 1.643744 -2.208878
1 -2.506316 0.130936 -3.095323
1 0.970056 3.268496 -3.467493

Co(H₂bim)₂(HBim)²⁺ Singlet

-1505.5420912 (0.503129)
 27 -0.026692 0.009421 -0.040056
6 1.610402 2.107252 -0.784330
6 0.788427 2.608319 0.311163
7 -0.097108 1.762868 0.784831
7 1.136969 0.924950 -1.300972
7 1.470928 -0.578498 1.021674

6 1.946201 -1.764499 0.732598
6 1.231166 -2.440111 -0.346131
7 0.247432 -1.737729 -0.849099
7 -1.582399 0.448788 -1.117131
6 -2.753540 0.139502 -0.624686
6 -2.702089 -0.580836 0.649531
7 -1.498671 -0.734982 1.137930
7 -3.703698 -1.161723 1.345145
1 -4.663969 -0.842953 1.288152
7 -3.817204 0.600646 -1.317624
1 -4.728844 0.160014 -1.272517
7 0.844079 3.784337 0.942839
1 1.339142 4.582763 0.564189
7 2.970300 -2.191731 1.499325
1 3.635363 -2.883472 1.172807
7 1.473225 -3.624995 -0.942585
1 1.942164 -4.389151 -0.470503
6 -0.300446 -2.492948 -1.978905
1 -1.393977 -2.545857 -1.925692
1 -0.029289 -1.983750 -2.915411
6 0.365058 -3.888464 -1.869221
1 -0.316116 -4.642173 -1.444487
1 0.742304 -4.256125 -2.831116
6 2.251505 -0.052368 2.146805
1 2.588617 0.970741 1.948292
1 1.621185 -0.036689 3.048476
6 3.432790 -1.044363 2.292744
1 4.366292 -0.641359 1.870912
1 3.613289 -1.339557 3.333331
6 -0.277513 3.873046 1.875024
1 0.049259 4.241365 2.855736
1 -1.049347 4.554709 1.484710
6 -0.770923 2.399027 1.921058
6 -1.801061 1.286774 -2.297769
1 -1.158537 0.974516 -3.127256
1 -1.540293 2.325431 -2.047142
6 -3.311333 1.125474 -2.594929
1 -3.501483 0.403571 -3.404893
1 -3.801048 2.073768 -2.846205
6 -1.625954 -1.567688 2.337884
1 -1.227519 -2.571988 2.124280
1 -1.050708 -1.149616 3.172555
6 -3.146899 -1.610340 2.627404
1 -3.506921 -2.615204 2.878806
6 3.105047 1.725888 -2.302855
1 2.878802 2.175955 -3.284722
1 4.191493 1.571436 -2.261600
6 2.270196 0.431372 -2.090508
1 2.858142 -0.326904 -1.542205
1 1.935744 -0.020981 -3.033431
7 2.675810 2.667037 -1.262746
1 -1.862139 2.328733 1.832416
1 -0.477364 1.904323 2.859722
1 -3.437410 -0.918922 3.433936

Co(H₂bim)₂(HBim)²⁺ Triplet
-1505.5408299 (0.500823)
27 0.012962 0.090382 -0.043184
 6 0.529112 2.690076 -0.776300
 6 -0.224864 2.797939 0.467862
 7 -0.617635 1.652655 0.968043
 7 0.715117 1.381339 -1.147727
 7 1.988481 -0.191726 1.098711
 6 2.712670 -1.054804 0.449142
 6 2.050399 -1.792341 -0.635550
 7 0.856069 -1.404122 -1.003281
 7 -2.013250 -0.120395 -1.060043
 6 -2.800323 -0.894580 -0.372304
 6 -2.218447 -1.517011 0.826094
 7 -0.989148 -1.196479 1.137600
 7 -2.798013 -2.441377 1.626047
 1 -3.804010 -2.512424 1.723452
 7 -4.093729 -0.973337 -0.782557
 1 -4.666346 -1.789460 -0.599501
 7 -0.537052 3.883949 1.181322
 1 -0.472388 4.824820 0.811952
 7 3.993831 -1.226984 0.865289
 1 4.720495 -1.537189 0.229771
 7 2.571554 -2.820434 -1.342669
 1 3.276915 -3.430210 -0.944747
 6 0.444290 -2.252615 -2.127865
 1 -0.571338 -2.634583 -1.976908
 1 0.443050 -1.654047 -3.050798
 6 1.505268 -3.377934 -2.180651
 1 1.135069 -4.321375 -1.749798
 1 1.868571 -3.575078 -3.196617
 6 2.861490 0.388504 2.125460
 1 2.809794 1.485031 2.098642
 1 2.508132 0.067747 3.118036
 6 4.283951 -0.154566 1.826443
 1 4.936517 0.604990 1.368838
 1 4.785077 -0.555707 2.716070
 6 -1.439969 3.483209 2.259854
 1 -1.135092 3.928105 3.215306
 1 -2.470145 3.802121 2.036210
 6 -1.286777 1.936507 2.241999
 6 -2.842463 0.479444 -2.110355
 1 -2.332943 0.447460 -3.081802
 1 -3.012538 1.539036 -1.860184
 6 -4.165368 -0.324929 -2.098303
 1 -4.203377 -1.080855 -2.899050
 1 -5.056072 0.310571 -2.172725
 6 -0.604409 -2.019067 2.289694
 1 0.098857 -2.796929 1.954926
 1 -0.098444 -1.416026 3.051637
 6 -1.931506 -2.632411 2.792646
 1 -1.842909 -3.695733 3.045998
 6 1.654916 2.959633 -2.627656
 1 1.188514 3.296604 -3.567120
 1 2.708217 3.276890 -2.676791
 6 1.488797 1.436897 -2.384294

 1 2.452435 0.920676 -2.256931
 1 0.950309 0.928981 -3.197702
 7 1.007230 3.642877 -1.513990
 1 -2.254802 1.425444 2.304451
 1 -0.659328 1.581962 3.074178
 1 -2.336978 -2.094604 3.664470

Co(H₂bim)₃²⁺ Quartet/Doublet MECP
-1506.167360
27 -0.0142556 0.0505601 0.0112698
 6 -2.2893149 -1.5197438 0.7974479
 6 -2.8627228 -0.7992775 -0.3491070
 7 -2.0651845 -0.0015510 -0.9985615
 7 -1.0632122 -1.2252300 1.1500159
 7 0.7640938 -1.4720362 -1.0518154
 6 1.9569769 -1.9068365 -0.7421684
 6 2.6819093 -1.2324770 0.3422738
 7 2.0303923 -0.3428337 1.0310507
 7 -0.5097361 1.6688950 1.0801587
 6 -0.1071121 2.8120004 0.5866099
 6 0.6287447 2.7119055 -0.6693840
 7 0.7906503 1.4925405 -1.1175312
 7 1.2290560 3.6953915 -1.3850177
 1 0.8650198 4.6415972 -1.3846338
 7 -0.4913370 3.9228850 1.2637119
 1 0.0558699 4.7756574 1.2278106
 7 -4.1268274 -0.9328990 -0.8350274
 1 -4.9062574 -1.2023179 -0.2467236
 7 2.4318630 -2.9255148 -1.5026632
 1 3.1127528 -3.5774150 -1.1297286
 7 3.9599788 -1.5069418 0.7284578
 1 4.6482096 -1.8202069 0.0524703
 6 2.9571670 0.1196135 2.0704162
 1 2.9655762 1.2161455 2.1256401
 1 2.6082552 -0.2546430 3.0464025
 6 4.3400197 -0.4752340 1.7011614
 1 5.0060868 0.2685825 1.2353346
 1 4.8600029 -0.9195760 2.5588559
 6 0.2932385 -2.2771947 -2.1841002
 1 -0.7278173 -2.6360927 -2.0103965
 1 0.2749813 -1.6490637 -3.0880721
 6 1.3185392 -3.4293055 -2.3132507
 1 0.9379246 -4.3753041 -1.8966472
 1 1.6362845 -3.6050994 -3.3482892
 6 -4.3163486 0.1140072 -1.8445097
 1 -4.8149758 -0.2879048 -2.7353118
 1 -4.9299212 0.9353060 -1.4405276
 6 -2.8519656 0.5459494 -2.1091069
 6 -1.3154960 1.9783944 2.2640581
 1 -1.0473767 1.3277647 3.1049490
 1 -2.3772067 1.8070257 2.0268718
 6 -1.0360516 3.4724172 2.5505963
 1 -0.2916594 3.6082719 3.3515367
 1 -1.9405395 4.0353168 2.8105479
 6 1.6426632 1.5884450 -2.3064309
 1 2.6477216 1.2146850 -2.0559254

```
1  1.2496324  0.9758272 -3.1263178      6 -0.6966414 -2.1445229  2.2336544
6  1.6714908  3.0960757 -2.6500578      1  0.0124893 -2.8902144  1.8427222
1  2.6713327  3.4540037 -2.9235000      1 -0.2009731 -1.6096298  3.0520403
6 -2.0272226 -2.7994689  2.6684650      7 -2.8711405 -2.5109138  1.5099741
1 -2.4453793 -2.3344648  3.5764070      1 -2.7353212  1.6360630 -2.1679843
1 -1.9416763 -3.8802550  2.8344900      1 -2.4732782  0.1238443 -3.0538250
1 -3.8657205 -2.6929516  1.5207726      1  0.9700807  3.3489906 -3.4612703
```